

## Research Article

# Plugging Performance of a New Sulfonated Tannin Gel System Applied in Tight Oil Reservoir

Tianhan Xu <sup>1</sup>, Jian Wang <sup>1</sup>, Zhiwen Bai <sup>2</sup>, Junheng Wang <sup>1</sup>, and Peng Zhao <sup>1</sup>

<sup>1</sup>State Key Laboratory of Oil and Gas Reservoir Geology and Exploitation, Southwest Petroleum University, Sichuan Province, China

<sup>2</sup>Baikouquan Oil Plant, Xinjiang Oilfield Company, CNPC, Karamay, Xinjiang 834000, China

Correspondence should be addressed to Jian Wang; 404674469@qq.com

Received 2 November 2021; Revised 5 March 2022; Accepted 22 March 2022; Published 23 April 2022

Academic Editor: Jinjie Wang

Copyright © 2022 Tianhan Xu et al. This is an open access article distributed under the Creative Commons Attribution License, which permits unrestricted use, distribution, and reproduction in any medium, provided the original work is properly cited.

In this study, based on the high-temperature characteristics of Western China tight oil reservoirs, a phenolic-larch tannin, temperature-resistant, plugging agent was synthesized by changing the mass fractions of larch tannin, double cross-linking agent, and accelerator. Young's modulus of the dispersed gel was directly measured by an atomic force microscope, and the macroscopic plugging performance was evaluated by a physical simulation experiment of the artificially fractured natural core from Western China tight oil oilfield, thereby establishing a mapping relationship between the two. Research indicates that the formula of the high-temperature-resistant tannin system optimized by the experiment is 3.0% sulfonated tannin + 3.0% formaldehyde cross-linking agent + 1.0% phenol cross-linking agent + 0.05%  $\text{MnSO}_4$  accelerator; the mechanical strength of the tannin gel and its plugging performance have a linear relationship. When Young's modulus rises from 18.74 to 63.89 KPa, the plugging rate rises from 94.11% to 97.44%.

## 1. Introduction

Given the increasing difficulty of conventional oil and gas exploration and development, the development of unconventional resources such as tight oil and gas has become inevitable [1, 2]. Tight oil storage and seepage conditions are poor, and fracturing is generally used to connect the pores in the reservoir and expand the seepage area. However, this mode of development will aggravate the difference in matrix-fracture seepage flow and form a flow channel. Therefore, after long-term fracturing development, reservoir regulation is required to change the original seepage channel, increase the swept volume, and achieve the purpose of increasing oil well production [3, 4]. Current research mostly uses polyacrylamide cross-linked polyvalent metal ion ( $\text{Cr}^{3+}$ ,  $\text{Al}^{3+}$ ,  $\text{Zr}^{4+}$ , etc.) gel to block gas flow channels [5, 6], but this gel is affected by high temperature and  $\text{Ca}^{2+}$  and  $\text{Mg}^{2+}$ , which will cause the plugging agent to fail. At present, there are few studies on organic cross-linking agent gels (formaldehyde, phenol, etc.), and most of them focus on the use of a single cross-linking agent to synthesize the gel

[7–9]. Compared with metal ions and a single organic cross-linking agent, double organic cross-linking agent gel has higher thermal stability through covalent bond cross-linking and is more suitable for high-temperature, unconventional oil reservoirs [10–12].

Due to the high temperature and high pressure of unconventional tight oil reservoirs in Xinjiang and the characteristics of ultralow porosity and ultralow permeability reservoirs, conventional plugging agents are difficult to plug, and the effective plugging time is not long, and the plugging effect is extremely poor. In this study, based on the high-temperature characteristics of the tight oil reservoirs in Xinjiang tight oil reservoir, a phenolic-larch tannin temperature-resistant plugging agent was synthesized by changing the mass fractions of larch tannin, double cross-linking agent, and accelerator.

Wang et al. [13–15] have made a high-temperature blocking agent capable of resisting 250°C by mixing sulfonated tannin extract with phenol, formaldehyde, or paraformaldehyde. Fangeng et al. [16] used tannin extract as raw material to react with phenol and formaldehyde and

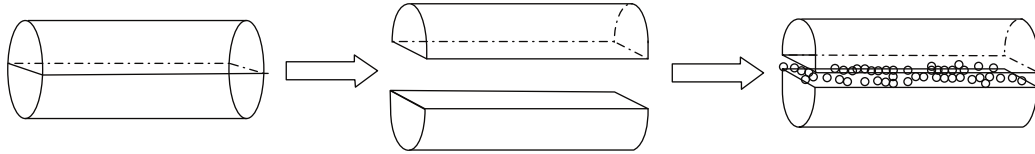


FIGURE 1: Physical treatment of natural cores.

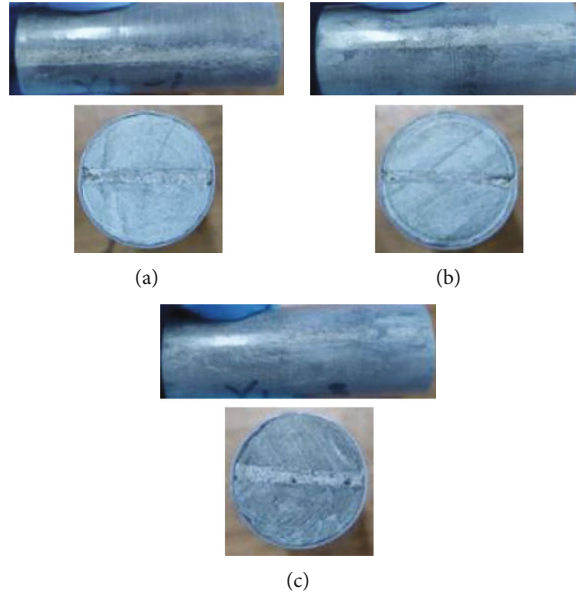


FIGURE 2: Artificially fractured natural core.

TABLE 1: Summary of physical properties of the cores applied in this study.

Core number	Length (cm)	Diameter (cm)	Porosity (%)	Permeability ( $10^{-3} \mu\text{m}^2$ )
Core #1	6.77	2.62	10.72	1726.1
Core #2	6.04	2.64	8.02	1688.3
Core #3	6.70	2.57	7.37	1696.3

then used transition metal salts such as inorganic salts  $\text{MnSO}_4$ ,  $\text{TiCl}_4$ , and tannin extract. The chelation reaction occurs to promote the cross-linking reaction, and the gel is formed in the range of  $170\sim 280^\circ\text{C}$  and pH value of  $4\sim 9$ , and a good blocking effect is achieved. Dezhi et al. [17] also used tannin extract as raw material to prepare a water plugging agent suitable for high-temperature profile control. It was determined by experiments that after adding an accelerator, a selective plugging agent with enhanced strength of the plugging agent can be obtained with the increase of temperature, which can be applied to high-temperature formations. Han et al. [18] have obtained a profile control and water plugging agent that can withstand high temperatures of  $300^\circ\text{C}$  through experimental research using tannin extract as raw material. After field tests in Liaohe Oilfield, they obtained a good production increase effect, and at the same time, the water yield also decreased.

Gel dispersion is obtained by shearing and grinding the synthesized gel to a state where the particles are stably dispersed in an aqueous solution [19]. The dispersed gel is easy to inject because it has low viscosity and controllable particle size; it can be elastically deformed, spontaneously aggregate in the pore throat, and migrate to the deep part of the reservoir [20–25], which can avoid the dilution of formation water during pumping and formation shearing and migration. Compared with other granular plugging control agents, dispersed gel has better stratum adaptability [26, 27].

Plugging performance is an important index to evaluate the application of gel dispersion in the oil field, which is mainly affected by the characteristics of the dispersed gel [28]. At present, research on the mechanical properties of gel-plugging agents mostly has involved the performance of large-particle-size gel [29–31]. The mechanical properties of dispersed gels have not been systematically studied. The ability of dispersed gels with different mechanical properties to resist deformation after being squeezed during the migration process is different, which affects the blocking effect. At present, the gel strength code (GSC) method and rheological parameter method are generally used to characterize the strength of bulk gel [32–34], but there are few studies on directly characterizing the mechanical properties of the dispersed gel itself. Therefore, this paper introduces micro-nano-scale Young's modulus, which reflects the ability of the dispersed gel to resist deformation after being

TABLE 2: Experiment reagents used in this study.

Base tannin	Cross-linking agent		Accelerator	pH conditioner
Larch tannin (tannin content 60%, nontannin content 35%, and insoluble matter content 5%)	Formaldehyde (analytical pure)	Phenol (analytical pure)	MnSO <sub>4</sub> (analytical pure)	Sodium hydroxide (analytical pure)



(a) YP-1 high-temperature, high-pressure gel performance test device



(b) Atomic force microscope

FIGURE 3: Instruments used in the experiment.

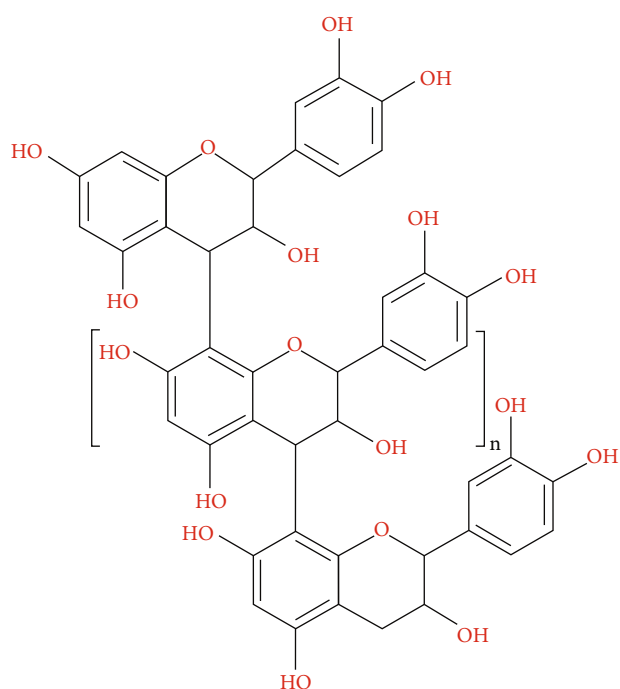


FIGURE 4: Polyprocyanidin [42].

compressed when it migrates in the porous medium and directly quantifies the mechanical properties of the gel. Traditional measurement methods of Young's modulus include the optical lever stretching method, pulse excitation method, and acoustic resonance method [35–37], but none of these methods can be used to characterize micro-nano-scale materials. With the development of nanomechanical measure-

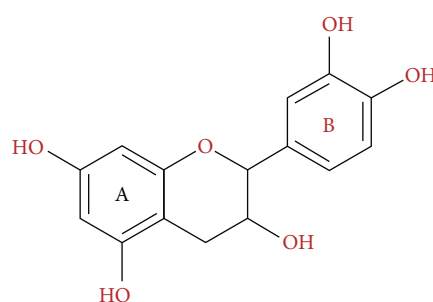


FIGURE 5: Procyanidin monomer [42].

ment technology, the atomic force microscope has become the most advanced and intuitive method for measuring small-scale materials [38–41].

Different from previous literature, the three new insights in this study mainly focus on the strengthening of the sulfonated larch gel structure system through the paraintermediate, the relationship between the gel storage modulus and Young's modulus of its dispersion, and the relationship between its mechanical strength and its macroscopic plugging performance. In this paper, by optimizing the mass fractions of four reagents (tannin, formaldehyde, phenol, and manganese sulfate) to synthesize temperature-resistant sulfonated larch gel, the relationship between the mechanical strength of sulfonated larch gel and the plugging performance was studied through three artificially fractured core flow experiments. The formula of the high-temperature-resistant tannin system optimized by the experiment is as follows: 3.0% sulfonated tannin + 3.0% formaldehyde cross-linking agent + 1.0% phenol cross-linking agent + 0.05% MnSO<sub>4</sub> accelerator. Secondly, the mechanical strength of the

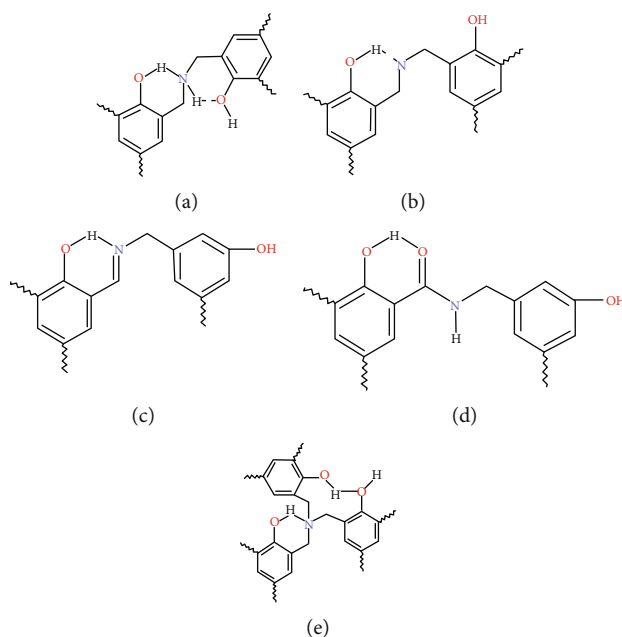


FIGURE 6: Structural intermediate in the cross-linking process.

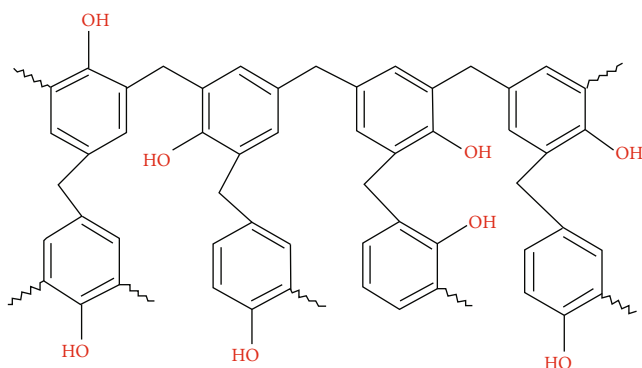


FIGURE 7: Novolac-type phenolic resin forms a network-like strengthening structure.

tannin gel and its plugging performance have a linear relationship. When Young's modulus rises from 18.74 to 63.89 kPa, the plugging rate rises from 94.11% to 97.44%.

## 2. Materials and Methods

**2.1. Materials.** In this study, artificially fractured natural cores (3.15 in) were used to conduct macroscopic plugging performance evaluation experiments. The cores were cut from the Xinjiang oilfield tight oil reservoir. The core was first cut in half along the midline and filled with quartz sand to simulate postfracturing fractures. Use a small amount of epoxy resin and heat-shrinkable tubing for fixing to ensure the overall strength of the core. The preparation process is shown in Figures 1 and 2. The properties (permeability and porosity) of the cores are listed in Table 1. The brine used in this study was simulated formation water. The salinity of the brine was 7197.77 mg/L.

The reagents used in this experiment are shown in Table 2.

The instruments used in this study were a JB200-SH electric stirrer (speed range of 0 to 8000 rpm); YP-1 high-temperature, high-pressure gel performance test device (Figure 3(a)); Keysight 7500 atomic force microscope (AFM) (Figure 3(b)); oven; electronic balance (accuracy of 0.001 g); and ground flask, beaker, dropper, suction ball, glass rod, graduated cylinder, etc.

### 2.2. Methods

**2.2.1. Preparation Principle of Larch Tannin Gel.** The main component of larch tannin is condensed tannin, its chemical composition is polyanthocyanidin, the average molecular weight is about 2800 (determined by vapor phase osmometry (VPO)), and the average degree of polymerization is 9 to 10. Its specific configuration is shown in Figures 4 and 5. Larch tannin has a higher molecular weight and a higher viscosity, and the length of the  $-\text{CH}_2-$  cross-linked bond generated by formaldehyde is not long enough to form sufficient cross-links between the reaction points, resulting in insufficient bonding strength. Therefore, a second cross-linking agent, phenol, was added in this study. The phenol molecules can react with the formaldehyde cross-linking agent in the main body of the gel-forming solution, and the formed structure can be interlaced with the main network structure formed by larch tannin to make the system whole. The structure is more compact, and the strength is greatly improved.

The reaction rate is significantly affected by temperature and accelerator. Therefore, an accelerator,  $\text{MnSO}_4$ , was added in this study to accelerate the reaction process, such that the main network structure formed by larch tannin and the novolac phenolic resin-reinforced structure were

TABLE 3: Observation method to evaluate gel standards.

Level	Status description	Classification
A	The gel viscosity is the same as the initial viscosity, and no gel is formed by visual inspection	No gel formed
B	The gel viscosity is slightly higher than the initial polymer viscosity	
C	Upside down has obvious flow	Weak gel
D	There is a small amount of gel that does not flow quickly	
E	The gel does not flow easily	
F	The gel can only flow in a small area at the top	Medium gel
G	The gel flow is about halfway down	
H	The surface of the gel is slightly deformed when inverted	
I	The surface of the gel is not deformed when inverted	Strong gel



FIGURE 8: Breakthrough vacuum experimental device [44].

formed almost at the same time and that their structures were intertwined to make the system whole. The overall structure was more compact, and the strength was greatly improved. It continued to decompose during the heating and curing process, and there may be a variety of ortho-to-position intermediate structures during the cross-linking process [43], as shown in Figure 6.

Under the application of high temperature, the various intermediates formed by the mixture system composed of low-molecular-weight oligomers and various hydroxymethyl phenols will gel, and various intermediates will exist in the main body of larch tannin. Interlacing each other in the network structure makes the overall structure of the system more compact and greatly improves the strength. Its possible reinforcement network configuration is shown in Figure 7.

### 2.2.2. Preparation and Characterization of Larch Tannin Gel.

The following steps were taken to prepare the larch tannin gel: Add the dry larch tannin powder to clear water at room temperature, stir with an electric stirrer for 2 hours to fully dissolve it, and prepare a 0.3% to 7% tannin solution. Add formaldehyde with a mass fraction of 2.2% to 3.6% to the tannin solution, stir it evenly, and let it stand for 10 minutes. Add 0.5% to 3.0% phenol to the tannin solution, and stir well. Add 0.01% to 0.1%  $\text{MnSO}_4$  with a mass fraction of 0.01% to 0.1%, stir evenly, and put it in a constant temperature oven at 248°F for 24 hours.

The strength grade of the gel in the ground bottle was observed by visual inspection (Table 3) and measured by the vacuum penetration method (Figure 8). A HAAKE MARS III rotational rheometer was used to measure the storage modulus,  $G'$ , of the gel. The gel was aged at 302°F

for 30 days, the change in gel strength grade was observed every day, and the change in storage modulus was measured by the rheological parameter method.

Gel strength was measured by the breakthrough vacuum method [44]. The experimental setup is shown in Figure 8. Connect the blue-cap bottle containing the gel to the vacuum breakthrough experimental device as shown in Figure 1; insert the tip of the 1 mL pipette 1 cm below the surface of the gel. Start the vacuum pump. Slowly adjust the knob to increase the vacuum degree of the system. When the air breaks through the gel, the maximum reading of the vacuum gauge on the vacuum gauge is the breakthrough vacuum degree of the gel. It is referred to as the BV (breakthrough vacuum) value; each sample is repeatedly measured 3 times. Its arithmetic mean is taken as its final BV value. The larger the BV value, the higher the strength, on the contrary, the lower the strength.

At room temperature, an appropriate amount of the bulk gel was transferred onto a mica sheet, and the sample was scanned using the tapping mode of an atomic force microscope to characterize the microscopic morphology of the gel.

### 2.2.3. Preparation of Dispersed Gel and Its Young's Modulus Measurement.

Gel with different mass fractions of the cross-linking agent and clean water was added to a colloid pulverizer at a ratio of 1 : 1, and the micro-nano-scale dispersed gel with similar particle size was obtained by controlling the rate and time of cyclic shearing.

The test probe model SCANASYST-FLUID was selected, the elastic constant was 0.7 N/m, the Thermal Tune method was used to correct the elastic coefficient, and the scan rate was set to 1 Hz. The peak force mode of the atomic force microscope was used to measure in a liquid environment, and the relationship curve between the force and the distance between the probe and the dispersed gel sample was obtained. The distance between the probe and the dispersed gel sample was equivalent to the deformation of the dispersed gel sample. By fitting and calculating the DMT mechanical model, Young's modulus ( $E$ ) of the micro-nano-scale dispersed gel could be obtained [45]:

$$F = \frac{4}{3} E \sqrt{R \delta_s^3} + F_a, \quad (1)$$

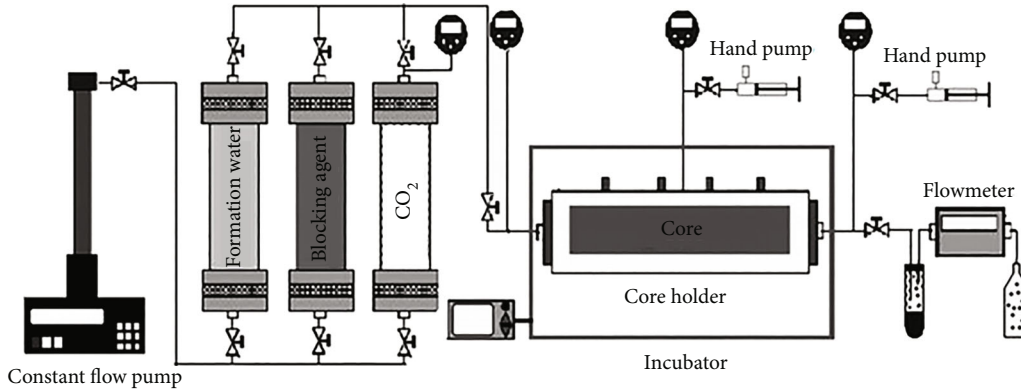


FIGURE 9: Single-core physical experiment flow chart.

where  $F$  is the force between the tip and the sample,  $E$  is the DMT modulus,  $R$  is the radius of the tip,  $\delta_s$  is the amount of sample deformation, and  $F_a$  is the adhesion force on the sample.

**2.2.4. Evaluation of the Plugging Performance of Dispersed Gel.** At room temperature, a single-core physical experiment was performed to determine the initial permeability of the natural core by water flooding. The dispersed gel was continuously injected into the natural core at a rate of 0.5 mL/min until the liquid injection volume reached 1 PV, and then, subsequent water flooding was performed at a constant speed until the pressure at the output end of the natural core was stable; the pressure change at the injection end of the natural core was recorded. The injection pressure, the plugging efficiency ( $\epsilon$ ), and the residual resistance coefficient ( $F_{rr}$ ) were used to characterize the plugging ability of the dispersed gel to the large pore throats in the reservoir. The flow chart of the experiment is shown in Figure 9.

### 3. Results and Discussion

#### 3.1. Gel Strength

**3.1.1. Effect of Tannin Concentration.** Tannin is the main body of the whole system, and its concentration directly affects the gel-forming performance of the plugging agent. Simulated formation water was used in the experiment to maintain the formaldehyde cross-linking agent concentration of 3.0%, the phenolic accelerator (P1) concentration of 1.5%, the inorganic salt accelerator concentration of 500 mg/L (unchanged), and the change in tannin concentration (0.3% to 7%). The experimental results were recorded and investigated for the gelation of the tannin system under different tannin concentrations. The experimental results are shown in Figure 10.

The experimental results show that a small amount of tannin does not gel. It can be gelatinized in the range of 0.3% to 7% by a mass fraction. When the mass fraction of the cross-linking agent is less than 0.3%, it is not enough to form a network structure with sufficient strength, but sporadic small micelles are formed, resulting in no gelling. As the concentration of tannin increases, the gelation time of

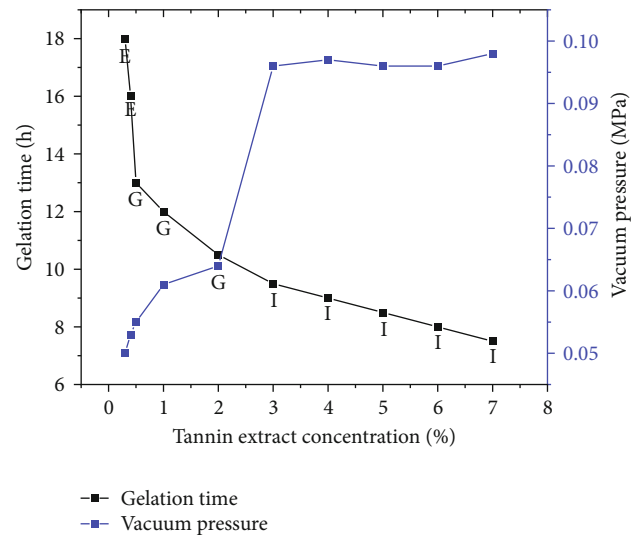


FIGURE 10: The effect of tannin concentration on the gel formation and strength of the system.

the system is gradually shortened, and the gel strength gradually increases. When the mass fraction reaches 3.0%, the gelation time of the entire system is 10 hours, the gel strength is level I, and the vacuum test can reach 0.095 MPa. Meeting the evaluation criteria and continuing to increase the tannin concentration, the gel strength does not change much, so the preferred tannin concentration is 3.0%, and the actual gel formation diagram is shown in Figure 11.

**3.1.2. Effect of Formaldehyde Cross-Linking Agent Concentration.** After keeping the temperature at 120°C, pH at 10 to 11, tannin concentration at 3.0%, phenol cross-linking agent concentration at 1.0%, and inorganic salt accelerator ( $\text{MnSO}_4$ ) concentration at 0.05% (unchanged) and changing the formaldehyde cross-linking agent concentration (2.2% to 3.6%), the experimental results were recorded and investigated for gel formation of the tannin system under different cross-linking agent concentrations. The experimental results are shown in Figure 12.

The experimental results show that the concentration of the formaldehyde cross-linking agent has a significant effect

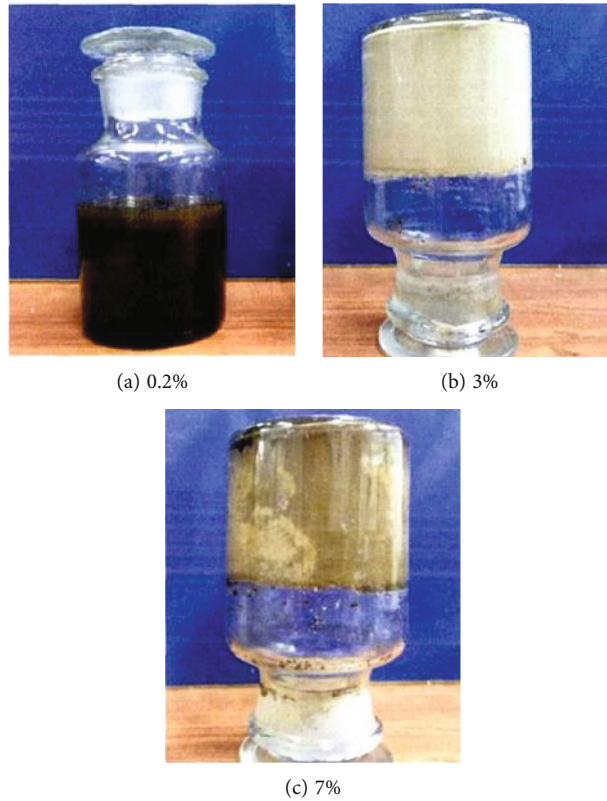


FIGURE 11: Performance of the gel under different tannin concentrations.

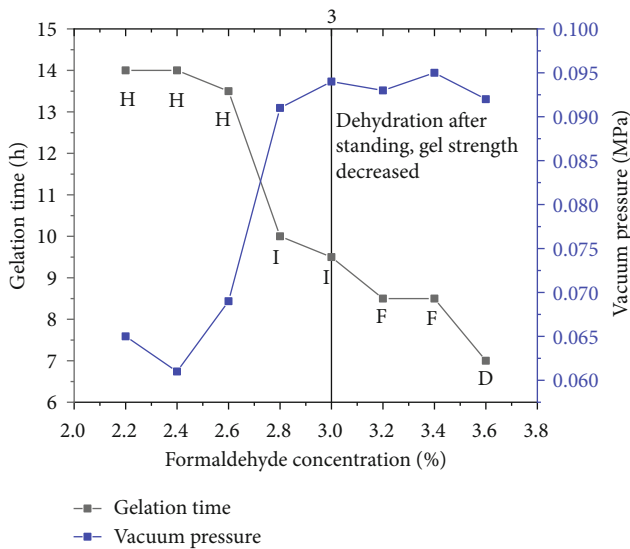


FIGURE 12: The effect of formaldehyde cross-linking agent concentration on the gel formation and strength of the system.

on the gel-forming effect of the entire system. As the concentration of the cross-linking agent increases, the gel-forming time gradually decreases, and the gel-forming strength first increases and then decreases. This is because when the concentration of tannin is constant, the number of reactive

groups is determined. As the concentration of the cross-linking agent increases, the reaction speed increases, the gel-forming time is shortened, and the gel strength increases. However, when the cross-linking agent concentration is too high, the system will be excessively cross-linked, the gel is easily dehydrated, and the strength becomes low. When the cross-linking agent concentration is 2.8% to 3.0%, the gel-forming time of the system is 9.5 hours, and the gel strength is level I, which meets the evaluation standard. Therefore, the preferred concentration of the formaldehyde cross-linking agent is 3.0%.

Experiments have found that when the content of the aldehyde cross-linking agent reaches 3.2% and above, the formed gel is prone to dehydration after a period of time, and then, the gel strength is greatly reduced. This phenomenon is caused by over-cross-linking of the cross-linking agent.

### 3.1.3. Effect of Phenol Cross-Linking Agent Concentration.

After keeping the tannin concentration at 3.0%, the formaldehyde cross-linking agent concentration at 3.0%, and the accelerator ( $MnSO_4$ ) concentration at 0.05% (unchanged) and changing the phenol concentration (0.5% to 3.0%), the experimental results were recorded and investigated for the gelation of the tannin system under different phenol cross-linking agent concentrations. The experimental results are shown in Figure 13.

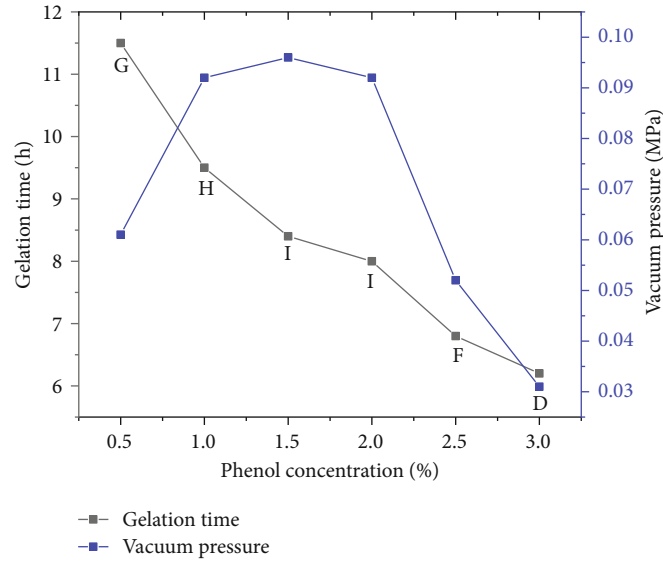


FIGURE 13: The effect of phenol cross-linking agent concentration on the gel formation and strength of the system.

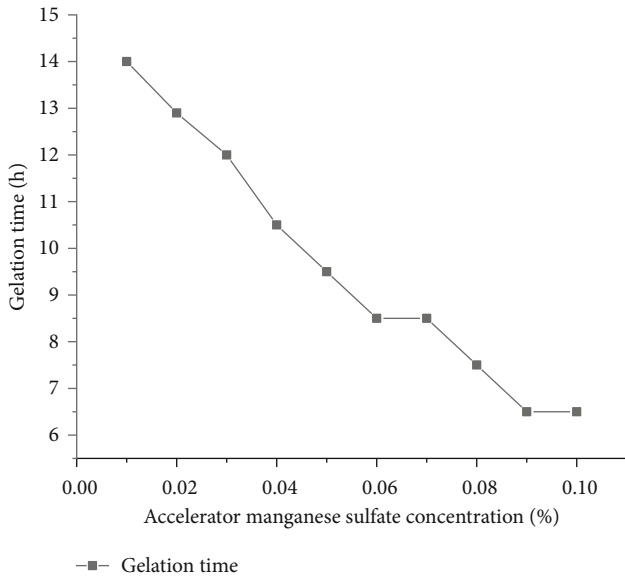


FIGURE 14: The effect of accelerator concentration on the gel-forming effect of the system.

The experimental results show that the performance of the plugging agent varies with the phenol cross-linking agent, similar to that of the formaldehyde cross-linking agent. When the concentration of the phenol cross-linking agent is less than 0.5%, the cross-linking strength of the system is too low; when the concentration is 1.0% to 2.0%, the greater the concentration of phenol cross-linking agent, the shorter the gelation time of the system and the stronger the gel formed. However, when its concentration exceeds 2.0%, the gel strength of the system is weakened because when the concentration of the phenol cross-linking agent is low, it cannot form an effective network structure with the sulfonated tannin and can only interact with the formaldehyde cross-linking agent at a local position. The interac-

tion of molecules involved in the cross-linking reaction results in poor gelation strength of the system. With the gradual increase in the concentration of the phenol cross-linking agent, more molecules can react with the formaldehyde cross-linking agent in the main body of the gel-forming solution, and the formed structure can be interlaced with the main network structure formed by the sulfonated tannin to make the system whole. The structure is tighter, and the strength gradually increases, but when the concentration of the phenol cross-linking agent exceeds a certain value, too many formaldehyde cross-linking agent molecules will preferentially react with the phenol cross-linking agent, weakening the main structure of the system and leading to a blocking agent. The strength is slightly reduced. Therefore, the concentration of the phenol cross-linking agent is preferably 1.0%.

**3.1.4. Effect of  $MnSO_4$  Accelerator Concentration.** After the sulfonated tannin reacted with phenol, the inorganic salt  $MnSO_4$  was used to chelate the tannin to promote the cross-linking reaction. In the experiment, Western China tight oilfield formation water was used to prepare the solution, keeping the tannin concentration at 3.0%, the formaldehyde cross-linking agent concentration at 3.0%, the phenol cross-linking agent concentration at 1.0%, and the accelerator concentration between 0.01% and 0.1%. The experimental results were recorded and investigated for the gelation of the tannin system under different accelerator concentrations. The experimental results are shown in Figure 14.

The experimental results show that as the concentration of the accelerator increases, the gelation time is gradually shortened, the gelation strength does not change much, and the strength level (I) basically remains unchanged because the transition metal salt has a chelation reaction with tannin to promote the cross-linking reaction. When the concentration of the cross-linking agent is constant,

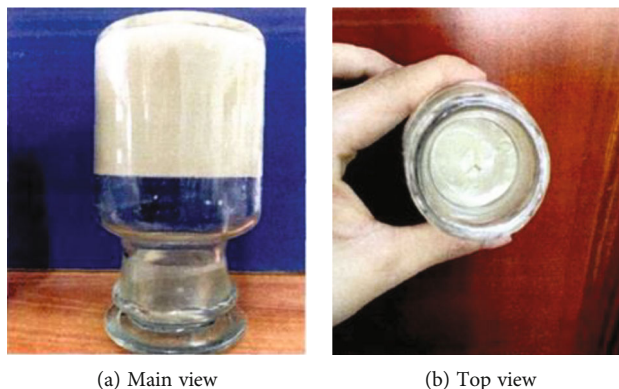


FIGURE 15: Preferred accelerator concentration tannin gel (accelerator 0.05%).

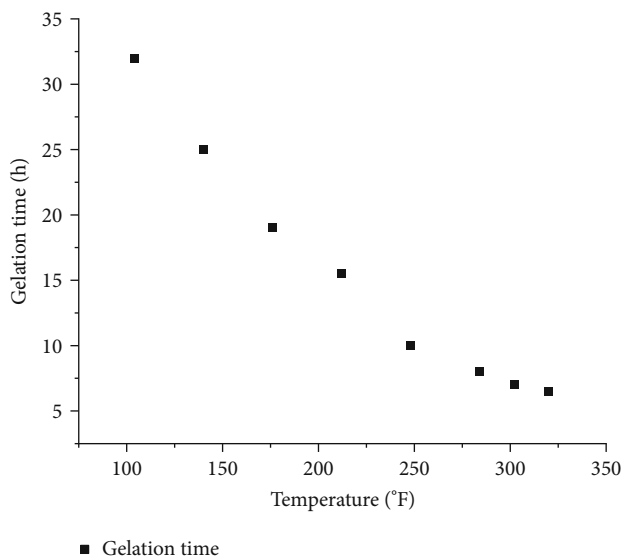


FIGURE 16: The effect of temperature on the gel-forming effect of the system.

adding the accelerator can increase the reaction speed of the system and shorten the gel-forming time. When the concentration of the accelerator is 0.05%, the gel-forming effect of the system meets the evaluation criteria. Considering the actual economic benefits, the preferred accelerator concentration is 0.05%. The actual gel-forming diagram is shown in Figure 15.

### 3.2. Gel Strength

#### 3.2.1. Effect of Temperature.

After taking the preferred formula (- 3.0% sulfonated tannin + 3.0% formaldehyde cross-linking agent + 1.0% phenol cross-linking agent + 0.05% accelerator) and placing it in a thermostat at different temperatures, the experimental results were recorded and investigated for the temperature resistance of the system. The gel was prepared at 104°F, 140°F, 176°F, 212°F, 248°F, 284°F, 302°F, and 320°F. The gelation time was used as an indicator to evaluate the gelling ability of the bulk gel. The results are shown in Figure 16. The experimental results show that the tannin

system cannot be gelled at 104°F. It can be gelled under the temperature conditions of 140°F to 320°F. When the temperature is between 140°F and 248°F, the strength of the gel is H grade, and when the temperature is before 248°F-320°F, the gel strength is I grade. As the temperature increases, the gelation time of the system decreases, indicating that the system has good temperature resistance stability.

3.2.2. Effect of Aging Time. The gel was aged at 302°F for 30 days. The storage modulus was used as an indicator to evaluate the stability of the bulk gel. The results are shown in Figure 17. The experimental results show that gels with 2.4% and 3.2% cross-linking agent mass fraction will decrease the mechanical strength of the gel to a certain extent as the aging time increases. The higher the cross-linking agent mass fraction, the more obvious the decrease in gel storage modulus. The storage modulus of the bulk gel with 3.0% tannin and 2.8% cross-linking agent mass fraction decreased from 2.74 to 2.54 Pa within 30 days. The storage modulus of the gel with 3.0% tannin and 3.0% cross-linking agent mass fraction decreased rapidly in the first 15 days (from 4.85 to 3.41 Pa); the later storage modulus decreased slightly and finally decreased to 3.13 Pa. However, the gel with 3.0% tannin and 3.2% cross-linking agent mass fraction was completely dehydrated when it was aged for 13 days. This shows that the dense structure in the gel can slow the release rate of bound water to a certain extent, but as the mass fraction of cross-linking agent increases, the degree of intermolecular cross-linking reaction increases. When the mass fraction of the cross-linking agent is too high, the formation reaction of multinuclear hydroxyl bridge ions moves relatively quickly to the right, resulting in excessive cross-linking. During a certain aging time, the spatial network structure of the gel system is destroyed due to syneresis, and the final strength is significantly reduced. Therefore, the gel with too high a mass fraction of cross-linking agent has poor stability and is not suitable for reasonable and effective control of the reservoir.

#### 3.2.3. Effect of pH Value.

After taking the preferred formula (- 3.0% sulfonated tannin + 3.0% formaldehyde cross-linking agent + 1.0% phenol cross-linking agent + 0.05% accelerator),

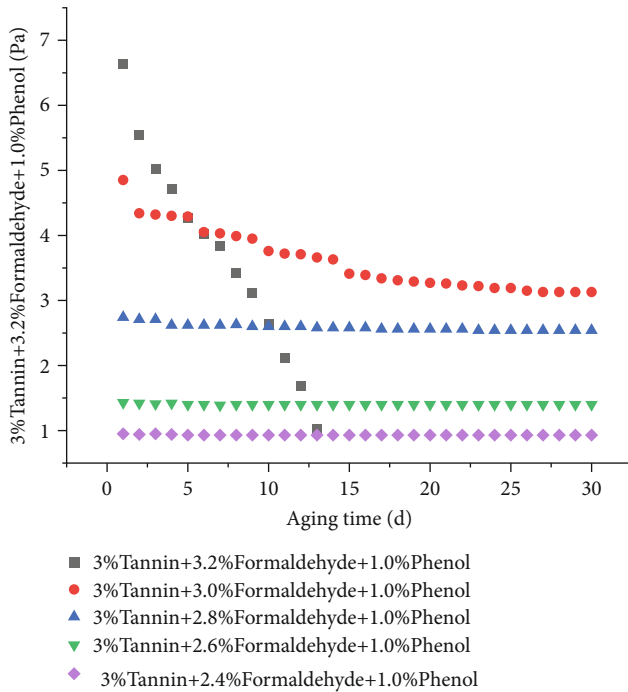


FIGURE 17: Change trend of gel strength with aging time.

adjusting the pH of the system, and placing it in a thermostat, the experimental results were recorded and investigated for the effect of pH on the performance of the tannin system. The experimental results are shown in Figure 18. With the increase in pH value, the gelation time of the tannin system gradually decreases, and the gel strength first increases and then decreases. This is because the B ring in the tannin system only reacts when the pH value is higher than 10 or in the presence of metal ions. A pH value higher than 10 will reduce the gelation time, and the network structure of the system will be affected in a strongly alkaline environment. If it is destroyed, it cannot be cross-linked or the cross-linked structure fails, which reduces the strength of the system. The experimental results also confirm this point; that is, under the same conditions as other components, without adjusting the pH value, the tannin solution (pH = 3 – 5) is not easy to gel, and the strength of the plugging agent is relatively weak.

The reaction of tannin and formaldehyde mainly occurs in the A ring, as shown in Figure 19(a). When the pH value is higher than 10, the B ring can react with formaldehyde [46], as shown in Figure 19(b).

Therefore, the suitable pH value of the tannin system is 6 to 10. At the same time, if the blockage needs to be removed at a later stage, an acid solution of pH < 5 or an alkaline solution of pH > 10 can be used to remove the blockage.

Through experimental screening, the final optimized formula of the high-temperature-resistant tannin system is as follows: 3.0% sulfonated tannin + 3.0% formaldehyde cross-linking agent + 1.0% phenol cross-linking agent + 0.05%  $\text{MnSO}_4$  accelerator.

**3.2.4. Effect of Erosion Resistance.** The core parameters used and the experimental results are shown in Table 4. The 6 PV

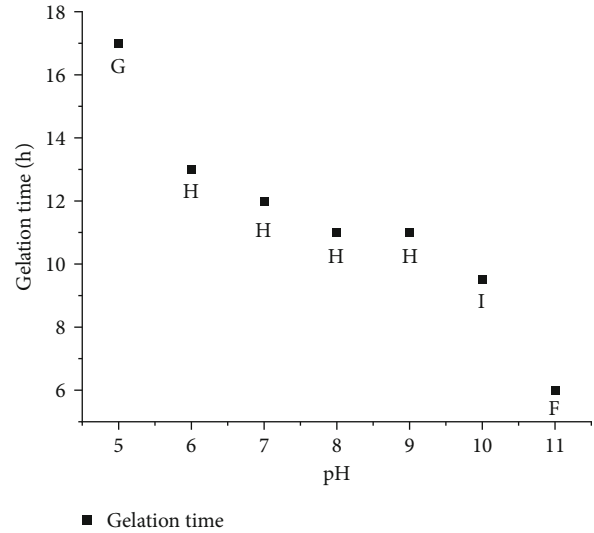


FIGURE 18: The change trend of gel strength with pH.

was continuously displaced by water injection at a constant flow rate, the pressure changes were recorded, and the scour resistance of the plugging agent was investigated. The variation of injection pressure with injection amount is shown in Figure 20.

The experimental results show that the injection pressure first increases and then decreases with the increase of the injected water. When the injection amount is 1.0 PV, the injection pressure reaches the maximum value, and the plugging rate can still reach 93.8% when the injection amount is 6 PV, indicating that the tannin extract system has good erosion resistance.

**3.3. Characterization of Young's Modulus of Dispersed Gel.** According to the gel-forming performance test results of the gel-forming liquid with different cross-linking agent concentrations, it was found that when the mass fraction of the sulfonated tannin is controlled at 3.0%, the mass fraction of the cross-linking agent increases from 2.2% to 2.4%, the macrostrength code assesses the gel at level H, and the storage modulus value measured by the rheological parameter method rises from 0.95 to 1.41 Pa. Then, the difference in the mechanical properties of the dispersion prepared by shearing the gel with the same strength code and different storage moduli will further increase, which will impact the effect of the dispersed gel in plugging the reservoir.

Therefore, Young's modulus ( $E$ ) of the dispersed gel was measured using the peak force mode of an atomic force microscope. Because the dispersed gel sample belongs to the state of soft particles and is dispersed in the liquid phase, a probe with a small elastic constant (1.0 N/m) was selected for measurement in a liquid environment. The force-distance curve of each pixel in the imaging process of the dispersed gel in a liquid environment was recorded in real time, and Young's modulus of the micro-nano-scale dispersed gel was obtained by fitting calculation. Because the micro-nano-scale dispersed gel particles were low-viscosity samples, there was a certain adhesive force when the needle tip interacted with the dispersed gel sample, but it was small.

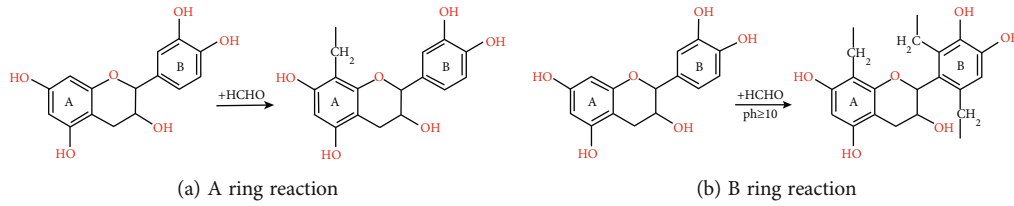


FIGURE 19: The reaction formula of tannin and formaldehyde.

TABLE 4: Erosion resistance performance evaluation test results.

Core number	Permeability ( $10^{-3} \mu\text{m}^2$ )	Injection blocking agent (PV)	After continuous displacement of 6 PV water permeability ( $10^{-3} \mu\text{m}^2$ )	Blocking rate (%)
Core #1	1726.1	0.5	106.5	93.8

Therefore, the Hertz model was not considered [47]. The JKR model under high adhesion experimental conditions is not suitable for characterizing Young’s modulus of dispersed gel [48]. Therefore, Young’s modulus of the micro-nano-scale dispersed gel was obtained by fitting the calculation of the DMT model [49]. During the experiment, parameter settings such as the peak force of each dispersed gel sample were always consistent with the test area.

Figure 21 shows the variation of the gel storage modulus and Young’s modulus of the dispersed gel with the mass fraction of the cross-linking agent. It can be seen from the figure that when the mass fraction of the cross-linking agent is between 2.4% and 3.2%, as the mass fraction of the cross-linking agent increases, Young’s modulus of the dispersed gel increases from 15.9 to 63.3 kPa, showing a linear increase. This trend is consistent with the change law of gel storage modulus on a macroscale. This linear increase law can be explained as when the mass fraction of the cross-linking agent increases, the cross-linking density between the polymer and the cross-linking agent increases greatly, the gel space network structure becomes denser, and the strength increases. The fracture of the prepared dispersed gel at the joint is relatively reduced, its phase deformation ability is reduced accordingly, and Young’s modulus of the dispersed gel measured under the same peak force increases.

Young’s modulus of micro-nano-scale dispersed gel is obviously higher than that of macroscale gel. The change in geometrical scale will lead to a significant increase in the order of molecules [50] and, at the same time, will increase the surface tension and thus change the mechanical properties of the sample. The storage modulus of the gel was measured by a dynamic shear rheometer under sinusoidal shear oscillation. It was used to indicate the storage of the gel’s shear deformation capacity, that is, the elasticity of the gel. Young’s modulus of the dispersed gel is measured by an atomic force microscope. The external load of atomic force microscopes (AFM) directly acts on the surface of the dispersed gel sample. Its Young’s modulus represents the ability

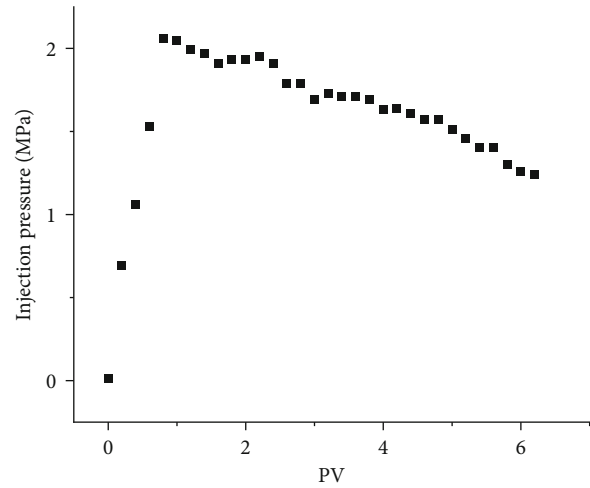


FIGURE 20: Plugging agent scour test.

of the dispersed gel to withstand unidirectional compressive stress and produce compression deformation.

The flexible particles of dispersed gel are not affected by the shear of the formation when they migrate in the porous medium and may be subjected to compression effects such as shape deformation when they pass through the pore throat [51]. When controlling the dominant channel and plugging the high-permeability layer, the gel may also be squeezed. Therefore, measuring Young’s modulus of the dispersed gel under compression can be used to effectively and quantitatively characterize its mechanical strength. Under the combined influence of the two factors of geometric scale and physical principle, the measured Young’s modulus of the dispersed gel and the storage modulus of the gel cannot be directly compared numerically, but there is a linear relationship between them.

### 3.4. Evaluation of the Plugging Performance of Dispersed Gel.

The artificially fractured core made from the natural core of the tight oil reservoir was used for physical simulation testing, and the prepared tannin dispersion was injected into the natural core. The injection pressure at a flow rate of 0.1 mL/min was investigated to characterize the injection performance and plugging performance of the dispersed gel. The change in the experimental residual resistance coefficient is shown in Table 3. When the mass fraction of the cross-linking agent increases from 2.6% to 2.8%, Young’s modulus of the dispersed gel rises from 18.74 to 36.06 kPa, indicating that the two systems have little difference. With the further increase of the mass fraction of the cross-

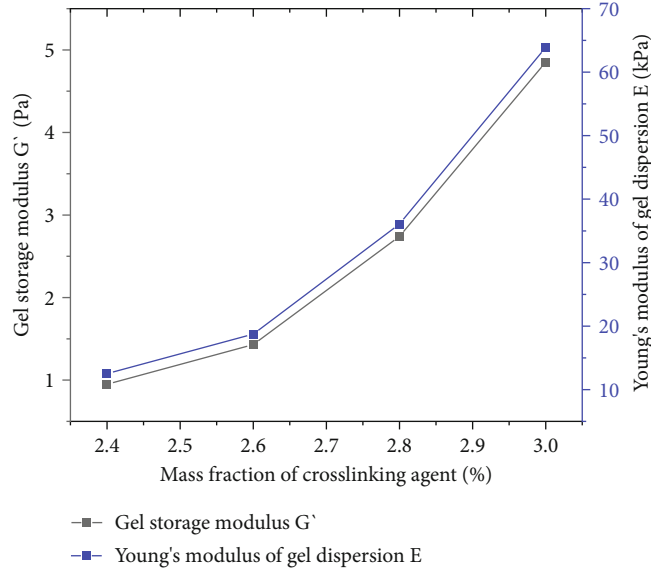


FIGURE 21: Variation of gel storage modulus and dispersed gel's Young's modulus with the mass fraction of cross-linking agent.

TABLE 5: Blocking rate of tannin plugging agent.

Core number	Mass fraction of formaldehyde (%)	Gel storage modulus $G'$ (Pa)	Young's modulus of dispersed gel $E$ (kPa)	$K_{w0}$ ( $10^{-3} \mu\text{m}^2$ )	$K_{w2}$ ( $10^{-3} \mu\text{m}^2$ )	Frr	Blocking rate (%)
Test #1	2.6	1.43	18.74	1726.1	101.8	16.95	94.11
Test #2	2.8	2.74	36.06	1688.3	87.8	19.22	94.82
Test #3	3.0	4.85	63.89	1696.3	43.3	39.17	97.44

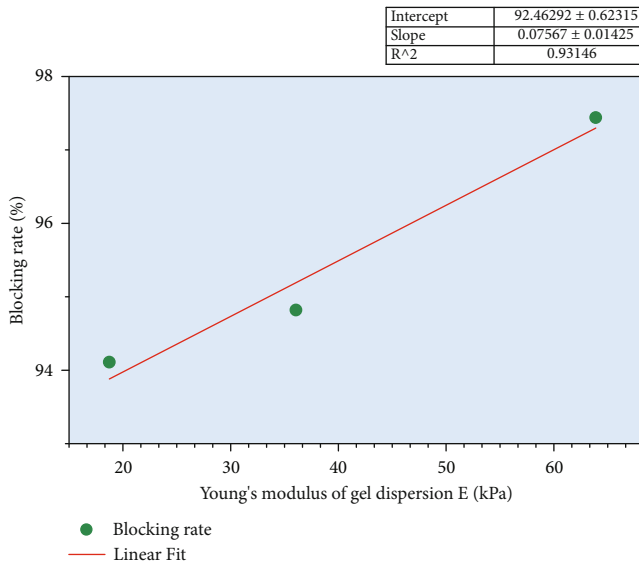


FIGURE 22: The plugging rate of dispersed gel varies with Young's modulus.

linking agent to 3.0%, Young's modulus of the dispersed gel increases relatively dramatically, and the residual drag coefficient also increases significantly. The experimental results are shown in Table 5. The plugging rate of different formulations of the plugging agent is above 94%, and the plugging rate of the preferred formulation is above 97%, indicating

that the tannin system has good plugging performance and can meet the needs of reservoirs. As shown in Figure 22, Young's modulus of the dispersed gel has a good linear relationship with the core plugging rate. Under the premise of ensuring the stability of the body gel, Young's modulus of the dispersed gel increases, and the plugging effect is better.

## 4. Conclusions

The conclusions of this study are listed as follows.

- (1) Through experimental screening, the final optimized formula of the high-temperature-resistant tannin system is 3.0% sulfonated tannin + 3.0% formaldehyde cross-linking agent + 1.0% phenol cross-linking agent + 0.05%  $\text{MnSO}_4$  accelerator
- (2) Young's modulus of the corresponding dispersed gel can be adjusted by adjusting the gel formula. When the mass fraction of tannin is 3.0% and the mass fraction of cross-linking agent increases from 2.4% to 3.0%, the cross-linking density increases, and the storage modulus of the gel increases from 1.43 to 4.85 Pa. Young's modulus of the dispersed gel obtained by physical shearing of the gel increases from 18.74 to 63.89 kPa
- (3) When Young's modulus of the dispersed gel increases from 18.74 to 63.89 kPa, the blocking rate

increases from 94.11% to 97.44%. Seeking the range of Young's modulus corresponding to excellent application performance of the dispersed gel provides a theoretical basis for improving the unconventional ability of dispersed gel to control tight oil reservoirs

## Data Availability

The data that support the findings of this study are available on request from the corresponding author. The data are not publicly available due to privacy or ethical restrictions.

## Conflicts of Interest

The authors declare that they have no conflicts of interest.

## Acknowledgments

This research was funded by the National Natural Science Foundation of China, grant number 52174035.

## References

- [1] C. Cheng, X. Li, and H. T. Qian, "Anisotropic failure strength of shale with increasing confinement: behaviors, factors and mechanism," *Materials*, vol. 10, no. 11, 2017.
- [2] Z. B. Zhang and X. Li, "The shear mechanisms of natural fractures during the hydraulic stimulation of shale gas reservoirs," *Materials*, vol. 9, no. 9, 2016.
- [3] X. Zhang and Y. Zhang, "Experimental and numerical investigation on basic law of dense linear multihole directional hydraulic fracturing," *Geofluids*, vol. 2021, Article ID 8355737, 19 pages, 2021.
- [4] J. Zou, Y.-Y. Jiao, F. Tan, J. Lv, and Q. Zhang, "Complex hydraulic-fracture-network propagation in a naturally fractured reservoir," *Computers and Geotechnics*, vol. 135, 2021.
- [5] B. J. Bai, J. Zhou, and M. F. Yin, "A comprehensive review of polyacrylamide polymer gels for conformance control," *Petroleum Exploration and Development*, vol. 42, no. 4, pp. 525–532, 2015.
- [6] Z. Dong, Y. Li, M. Lin, and M. Li, "Rheological properties of polymer micro-gel dispersions," *Petroleum Science*, vol. 6, no. 3, pp. 294–298, 2009.
- [7] T. Ichibouji, T. Miyazaki, E. Ishida et al., "Influence of cross-linking agents on apatite-forming ability of pectin gels," *20th International Symposium on Ceramics in Medicine*, vol. 361, pp. 559–562, 2007.
- [8] V. Purcar, D. Donescu, M. Ghiurea, S. Serban, C. Petcu, and C. Podina, "The effect of different cross-linking agents on the properties of hybrid films," *Optoelectronics and Advanced Materials-Rapid Communications*, vol. 3, no. 3, pp. 204–209, 2009.
- [9] H. Yamamoto, Y. Hirata, and H. Tanisho, "Cross-linking and insolubilization studies of water-soluble poly(l-ornithine)," *International Journal of Biological Macromolecules*, vol. 16, no. 2, pp. 81–85, 1994.
- [10] C. Anger, F. Deubel, S. Salzinger et al., "Organic-inorganic hybrid nanoparticles via photoinduced micellation and siloxane core cross-linking of stimuli-responsive copolymers," *ACS Macro Letters*, vol. 2, no. 2, pp. 121–124, 2013.
- [11] T. Liang, Z. Fan, Q. Liu, J. Wang, and J. Xu, "The study on double cross-linking gel plugging system," *IOP Conference Series: Materials Science and Engineering*, vol. 274, no. 1, 2017.
- [12] X. Wei, X. Li, X. Xue, and L. Ding, "Preparation and laboratory evaluation of a new type of cross-linking agent for acid fracturing fluid system," *Advanced Materials Research*, vol. 347, pp. 995–1000, 2011.
- [13] L. H. Wang, H. F. Xia, P. H. Han et al., "Synthesis of new PPG and study of heterogeneous combination flooding systems," *Journal of Dispersion Science and Technology*, vol. 43, no. 2, pp. 164–177, 2022.
- [14] X. Han, L. H. Wang, H. F. Xia, P. Han, R. Cao, and L. Liu, "Mechanism underlying initiation of migration of film-like residual oil," *Journal of Dispersion Science and Technology*, 2021.
- [15] H. F. Xia, L. H. Wang, P. H. Han, R. Cao, S. Zhang, and X. Sun, "Microscopic residual oil distribution characteristics and quantitative characterization of producing degree based on core fluorescence analysis technology," *Geofluids*, vol. 2021, Article ID 8827721, 17 pages, 2021.
- [16] C. Fangeng, H. Ling, and M. Baoqi, "Preparation of modified rubber bowl tannin extract for high temperature blocking agent," *Journal of Xi'an Shiyou University*, vol. 1, pp. 67–73, 1990.
- [17] L. Dezhi, Y. Fei, W. Rongjun, and D. Ming, "Study on high temperature blocking agent of larch tannin extract," *Xinjiang Oil and Gas*, vol. 8, Supplement 1, pp. 82–89, 2012.
- [18] X. Han, I. Kurnia, Z. Chen, J. Yu, and G. Zhang, "Effect of oil reactivity on salinity profile design during alkaline-surfactant-polymer flooding," *Fuel*, vol. 254, article 115738, 2019.
- [19] X. Sun, J. Zhao, T. Chen, and X. Liu, "Colloidal particle size of fumed silica dispersed in solution and the particle size effect on silica gelation and some electrochemical behaviour in gelled electrolyte," *Journal of Solid State Electrochemistry*, vol. 20, no. 3, pp. 657–664, 2016.
- [20] A. J. Gravelle and A. G. Marangoni, "Effect of matrix architecture on the elastic behavior of an emulsion-filled polymer gel," *Food Hydrocolloids*, vol. 119, article 106875, 2021.
- [21] M. T. Lopez-Lopez, L. Y. Iskakova, and A. Y. Zubarev, "To the theory of shear elastic properties of magnetic gels," *Physica A: Statistical Mechanics and its Applications*, vol. 486, pp. 908–914, 2017.
- [22] J. Q. Leng, M. Z. Wei, and B. J. Bai, "Review of transport mechanisms and numerical simulation studies of preformed particle gel for conformance control," *Journal of Petroleum Science and Engineering*, vol. 206, article 109051, 2021.
- [23] I. Kurnia, G. Y. Zhang, X. Han, and J. Yu, "Zwitterionic-anionic surfactant mixture for chemical enhanced oil recovery without alkali," *Fuel*, vol. 259, 2020.
- [24] Z. Chen, X. Han, I. Kurnia, J. Yu, G. Zhang, and L. Li, "Adoption of phase behavior tests and negative salinity gradient concept to optimize Daqing oilfield alkaline-surfactant-polymer flooding," *Fuel*, vol. 232, pp. 71–80, 2018.
- [25] A. M. S. Lala and N. A. A. El-Sayed, "Controls of pore throat radius distribution on permeability," *Journal of Petroleum Science and Engineering*, vol. 157, pp. 941–950, 2017.
- [26] S. M. Lin and L. X. Gu, "Influence of crosslink density and stiffness on mechanical properties of type I collagen gel," *Materials*, vol. 8, no. 2, pp. 551–560, 2015.

- [27] Y. Qin, R. Q. Liao, S. S. Luo, and J. Li, "The thermal gelation behavior and performance evaluation of high molecular weight nonionic polyacrylamide and polyethyleneimine mixtures for in-depth water control in mature oilfields," *Materials*, vol. 13, no. 18, 2020.
- [28] S. Zhao, D. Zhu, and B. Bai, "Experimental study of degradable preformed particle gel (DPPG) as temporary plugging agent for carbonate reservoir matrix acidizing to improve oil recovery," *Journal of Petroleum Science and Engineering*, vol. 205, article 108760, 2021.
- [29] R. Pandey and J. C. Conrad, "Gelation in mixtures of polymers and bidisperse colloids," *Physical Review E*, vol. 93, no. 1, 2016.
- [30] Y. Yao, M. Wei, and W. Kang, "A review of wettability alteration using surfactants in carbonate reservoirs," *Advances in Colloid and Interface Science*, vol. 294, 2021.
- [31] Y. Yao, M. Wei, and B. Bai, "Descriptive statistical analysis of experimental data for wettability alteration with surfactants in carbonate reservoirs," *Fuel*, vol. 310, article 122110, 2022.
- [32] J. Fang, J. Wang, Q. Wen et al., "Research of phenolic crosslinker gel for profile control and oil displacement in high temperature and high salinity reservoirs," *Journal of Applied Polymer Science*, vol. 135, no. 14, article 46075, 2018.
- [33] L. Romero-Zeron, F. Manalo, and A. Kantzas, "Characterization of crosslinked gel kinetics and gel strength by use of NMR," *SPE Reservoir Evaluation & Engineering*, vol. 11, no. 3, pp. 439–453, 2008.
- [34] S. Zhang, J. Guo, Y. Gu, Q. Zhao, R. Yang, and Y. Yang, "Polyacrylamide gel formed by Cr(III) and phenolic resin for water control in high-temperature reservoirs," *Journal of Petroleum Science and Engineering*, vol. 194, article 107423, 2020.
- [35] D. Hou, W. Zhang, P. Wang, M. Wang, and H. Zhang, "Mesoscale insights on the structure, mechanical performances and the damage process of calcium-silicate-hydrate," *Construction and Building Materials*, vol. 287, article 123031, 2021.
- [36] K. Mayumi, C. Liu, Y. Yasuda, and K. Ito, "Softness, elasticity, and toughness of polymer networks with slide-ring crosslinks," *Gels*, vol. 7, no. 3, p. 91, 2021.
- [37] I. Zafeiri, A. Beri, B. Linter, and I. Norton, "Mechanical properties of starch-filled alginate gel particles," *Carbohydrate Polymers*, vol. 255, article 117373, 2021.
- [38] S. Backes and R. von Klitzing, "Nanomechanics and nanorheology of microgels at interfaces," *Polymers*, vol. 10, no. 9, 2018.
- [39] A. Tanaka, H. Nakashima, Y. Kashimura, and K. Sumitomo, "Fabrication of a gel-supported lipid membrane array on a silicon substrate," *Japanese Journal of Applied Physics*, vol. 53, no. 1, 2014.
- [40] G. Li, J. Zhang, and X. Sun, "Preparation of superhydrophilic polyethersulfone by sol-gel method," *Advanced Materials Research*, vol. 785-786, pp. 1547–1550, 2013.
- [41] N. Wu, L. Chen, Q. Wei, Q. Liu, and J. Li, "Nanoscale three-point bending of single polymer/inorganic composite nanofiber," *Journal of the Textile Institute*, vol. 103, no. 2, pp. 154–158, 2012.
- [42] Y. Zhao and N. Yan, "Recent development in forest biomass derived phenol formaldehyde (PF) resol resin for wood adhesives application," *Journal of Biobased Materials and Bioenergy*, vol. 8, no. 5, pp. 465–480, 2014.
- [43] M. Derradji, J. Wang, and W. Liu, "X-functional phthalonitrile monomers and polymers," in *Phthalonitrile Resins and Composites*, pp. 107–174, Elsevier B.V, 2018.
- [44] Z. Hongtao, J. Han, C. Jinyuan, L. Xuehui, Z. Yanguang, and J. Kunpeng, "Viscosity quantitative breakthrough vacuum degree method for rapid determination of jelly strength," *Petroleum Drilling and Production Technology*, vol. 37, no. 5, pp. 116–119, 2015.
- [45] M. Satheesh Chandran and C. P. Reghunadhan Nair, "Maleimide-based Alder-Enes," in *Handbook of Thermoset Plastics*, pp. 459–510, Elsevier B.V, 2014.
- [46] J. Li, C. Li, W. Wang, W. Zhang, and J. Li, "Reactivity of larch and valonia tannins in synthesis of tannin-formaldehyde resins," *BioResources*, vol. 11, no. 1, pp. 2256–2268, 2016.
- [47] E. Dintwa, E. Tijskens, and H. Ramon, "On the accuracy of the Hertz model to describe the normal contact of soft elastic spheres," *Granular Matter*, vol. 10, no. 3, pp. 209–221, 2008.
- [48] I. I. Argatov, G. S. Mishuris, and V. L. Popov, "An approximate JKR model of elliptical contact between thin incompressible elastic coatings covering rigid cylinders," *Tribology Letters*, vol. 64, no. 1, 2016.
- [49] S. N. Ramakrishna, P. C. Nalam, L. Y. Clasohm, and N. D. Spencer, "Correction to study of adhesion and friction properties on a nanoparticle gradient surface: transition from JKR to DMT contact mechanics," *Langmuir*, vol. 35, no. 34, pp. 11242–11242, 2019.
- [50] E. Masoero, E. Del Gado, R. J. M. Pellenq, S. Yip, and F.-J. Ulm, "Nano-scale mechanics of colloidal C-S-H gels," *Soft Matter*, vol. 10, no. 3, pp. 491–499, 2014.
- [51] W. Zhao, H. Liu, J. Wang et al., "Investigation of restarting pressure gradient for preformed particle gel passing through pore-throat," *Journal of Petroleum Science and Engineering*, vol. 168, pp. 72–80, 2018.